



# Mercurochrome sensitized ZnO/In<sub>2</sub>O<sub>3</sub> photoanode for dye sensitized solar cell

Shital D. Satpute,<sup>§,1</sup> Jyoti S. Jagtap,<sup>§,1</sup> Pankaj K. Bhujbal,<sup>1</sup> Shital M. Sonar,<sup>2</sup> Prashant K. Baviskar,<sup>3</sup> Sandesh R. Jadker<sup>1</sup> and Habib M. Pathan<sup>1,\*</sup>

## Abstract

Here we fabricated a novel mercurochrome (MC) sensitized ZnO/In<sub>2</sub>O<sub>3</sub> photoanode based dye-sensitized solar cell (DSSC). The compact layer of ZnO was deposited on the substrate using a successive ionic layer adsorption and reaction (SILAR) method. Seed layers of ZnO/In<sub>2</sub>O<sub>3</sub> were deposited by a simple and low-cost Doctor-blade method. Deposited bilayered photoanode was studied to develop a cost-effective alternative photoanode and enhance the performance of ZnO based DSSCs. MC dye was used as photosensitizers to sensitized ZnO/In<sub>2</sub>O<sub>3</sub> photoanode. The obtained UV-Visible absorption spectra show that visible light absorption of the ZnO/In<sub>2</sub>O<sub>3</sub> bilayer photoanode was more effective than bare ZnO and In<sub>2</sub>O<sub>3</sub> photoanodes. The optical band gap was found to be 3.2, 2.87 and 2.95 eV for ZnO, In<sub>2</sub>O<sub>3</sub>, and ZnO/In<sub>2</sub>O<sub>3</sub> bilayer, respectively. A photoconversion efficiency of about 0.51 % was achieved for MC sensitized ZnO/In<sub>2</sub>O<sub>3</sub> bilayered photoanode based DSSC under 1 sun equivalent illumination. We confirm that ZnO/In<sub>2</sub>O<sub>3</sub> bilayer photoanode based DSSCs show a better performance than single-layered ZnO and single-layered In<sub>2</sub>O<sub>3</sub> based DSSCs.

**Keywords:** Dye-sensitized solar cell (DSSC); ZnO; In<sub>2</sub>O<sub>3</sub>; Bilayer film; Doctor Blade method; Mercurochrome (MC).

Received: 31 July 2020; Accepted: 14 September 2020.

Article type: Research article.

## 1. Introduction

The dye-sensitized solar cell (DSSC) offers an efficient, organic-inorganic, clean hybrid, and low-cost technology for future energy supply.<sup>[1]</sup> It is one of the promising third-generation solar cells. It provides better power conversion efficiency at low-cost material and low manufacturing costs compared to other solar cells. It offers one of the best challenges to other photovoltaic cells due to its excellent properties like semi-transparency, higher flexibility, low fabrication cost, and environmentally friendly.<sup>[2-3]</sup> Better performance of the DSSCs under diffused lights makes them an excellent choice for indoor applications.<sup>[4]</sup> There are four main parts of the DSSC, which include sensitized dye, a metal oxide semiconductor, redox couple electrolyte, and

counter electrode.<sup>[5]</sup> A dye should have strong absorption in the visible range and near IR region. Nano-sized particles of the metal oxide semiconductor are deposited on a transparent conducting oxide (TCO) like fluorine-doped tin oxide and indium-doped tin oxide, whose thickness should be in the order of 10-13 μm.<sup>[6]</sup> Metal oxide semiconductors are wide bandgap materials. It provides a high surface area for the absorption of dye molecules.<sup>[7]</sup> Metal oxides such as titanium oxide (TiO<sub>2</sub>),<sup>[8-12]</sup> zinc oxide (ZnO),<sup>[13]</sup> niobium oxide (Nb<sub>2</sub>O<sub>5</sub>),<sup>[14]</sup> tungsten oxide (WO<sub>3</sub>)<sup>[15]</sup> and tin oxide (SnO<sub>2</sub>)<sup>[16-18]</sup> are widely studied materials for the fabrication of DSSCs.<sup>[19]</sup>

Generally, TiO<sub>2</sub> is one of the extensively studied metal oxides due to its potential optical and electronic properties. The large surface area of TiO<sub>2</sub> increases the adsorption of dye molecules, which is helpful to enhance the photoconversion efficiency of the DSSCs.<sup>[20]</sup> The hopping mechanism is responsible for the conduction of electron from TiO<sub>2</sub> material. It limits efficient charge transfers from the TiO<sub>2</sub>.<sup>[21]</sup> ZnO is one of the promising alternatives to TiO<sub>2</sub> because of the abundance of zinc source, non-toxicity, low production cost, etc.<sup>[22]</sup> ZnO is an inorganic semiconductor material with a direct bandgap energy 3.37 eV and a large excitation energy

<sup>1</sup> Advanced Physics Laboratory, Department of Physics, Savitribai Phule Pune University, Pune-411007

<sup>2</sup>Department of Physics, S.V.S.'s Dadasaheb Rawal College, Dondaicha – 425 408

<sup>3</sup>Department of Physics, S N Arts, D J Malpani Commerce & B N Sarda Science College, Sangamner-422605 (MS)

\*E-mail: [pathan@physics.unipune.ac.in](mailto:pathan@physics.unipune.ac.in) (H. M. Pathan)

<sup>§</sup> Author contributed equally

of 60 meV at room temperature.<sup>[6,23-24]</sup>  $\text{In}_2\text{O}_3$  is a n-type semiconductor material having a wide band gap. It has an indirect band gap of 2.7 eV and a direct band gap of 3.6 eV. It is suitable as a photoanode in DSSCs. Fig. 1 shows the band diagram and electron transport mechanism of  $\text{ZnO}/\text{In}_2\text{O}_3$  photoanode based DSSC.

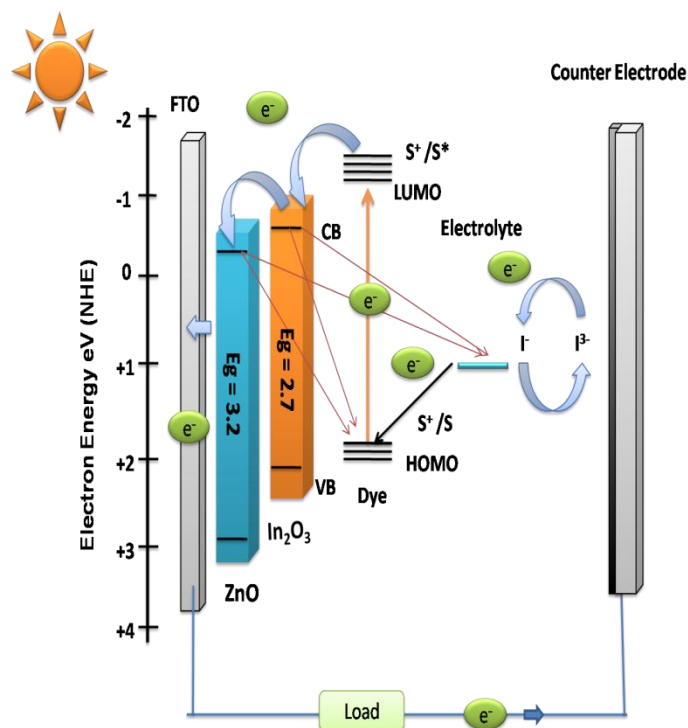


**Fig. 1** Band diagram & electron transport in  $\text{ZnO}/\text{In}_2\text{O}_3$  photoanode based DSSC.

There is a lot of research done on  $\text{ZnO}$  based DSSCs. To enhance the photoconversion efficiencies of the DSSCs, many researchers studied bilayered  $\text{ZnO}$  based photoanodes.<sup>[25,26]</sup> Aprilia *et al.*<sup>[27]</sup> reported  $\text{ZnO}/\text{TiO}_2$  bilayer heterojunction as a working electrode in Quasi solid dye sensitized solar cells. The highest efficiency achieved for the undoped  $\text{ZnO}/\text{TiO}_2$  photoanode was ( $\eta=0.67\%$ ). Sanctis *et al.*<sup>[28]</sup> reported stacked  $\text{In}_2\text{O}_3/\text{ZnO}$  heterostructures as semiconductors in thin film transistor devices. Zhang *et al.* achieved open-circuit voltage ( $V_{oc}$ ) of 0.34 V for  $\text{In}_2\text{O}_3$  based DSSC.<sup>[29]</sup> Eguchi *et al.* fabricated N3 sensitized  $\text{In}_2\text{O}_3$  based DSSC by the doctor blade method; and achieved 0.029 % efficiency.<sup>[30]</sup> Another researcher reported 0.32% photoconversion efficiency for MC sensitized  $\text{In}_2\text{O}_3$  based DSSC by the doctor blade method.<sup>[31]</sup> Till date,  $\text{ZnO}/\text{In}_2\text{O}_3$  bilayer photoanode based DSSCs are not studied. An additional layer of  $\text{In}_2\text{O}_3$  on the  $\text{ZnO}$  layer is attributed to the enhanced dye absorption rate and reduced electron recombination rate. This is responsible for the improvement in the photoconversion efficiency of the device.<sup>[32]</sup> A similar study was carried out by Beedri *et al.*<sup>[33]</sup> reporting that an additional layer of  $\text{Nb}_2\text{O}_5$  enhanced the performance of  $\text{ZnO}$  based DSSCs.

In present work, we have fabricated a novel mercurochrome (MC) dye-sensitized  $\text{ZnO}/\text{In}_2\text{O}_3$  photoanode for DSSC. The  $\text{ZnO}$  compact layer was deposited on the substrate using a SILAR method. A bilayer photoanode composed of an upper-layer of  $\text{In}_2\text{O}_3$  and a lower-layer of  $\text{ZnO}$  nanoparticles has been successfully deposited by a simple doctor blade method. Deposited bilayered photoanode was studied to develop a cost-effective alternative photoanode and enhance the performance of  $\text{ZnO}$  based DSSCs. MC dye was used as photosensitizers to sensitize  $\text{ZnO}/\text{In}_2\text{O}_3$  photoanode. We have studied structural, morphological, optical, and photovoltaic properties of  $\text{ZnO}/\text{In}_2\text{O}_3$  bilayer considering their applications for 3<sup>rd</sup> generation solar cells.

## 2. Experimental

### 2.1 Materials and Methods

The following materials and methods were used for the fabrication of  $\text{ZnO}/\text{In}_2\text{O}_3$  photoanode based DSSCs.

Materials: Zinc nitrate (Sigma Aldrich), aqueous ammonia, ethyl cellulose (SDFCL),  $\alpha$ -terpineol (HPCL), acetylacetone (SRL), etc.

Methods: (a) SILAR method for the deposition of a compact layer, (b) Doctor blade method for the deposition of seed layers of  $\text{ZnO}$  and  $\text{In}_2\text{O}_3$ .

### 2.2 Preparation of compact ZnO using SILAR method

The simple and cost-effective chemical route is Successive Ionic Layer Adsorption and Reaction (SILAR) method, which was used for the synthesis of  $\text{ZnO}$  compact layer. There are several advantages of the SILAR method such as low deposition temperature that avoids high-temperature effects, and good growth rate. This growth rate can be easily controlled by varying pH, the concentration of the solvent, deposition time. Fig. 2 shows a schematic representation of the SILAR method.

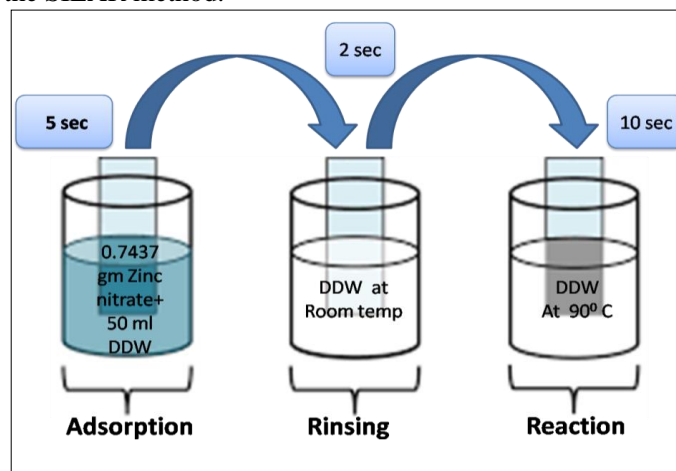


**Fig. 2** Schematic representation of the SILAR method.

There were three steps in one cycle (a) The immersion of the FTO into the first reactant containing the aqueous cationic precursor, (b) Rinsed with cold water, (c) dipped in

hot water. 25 SILAR cycles were repeated for the deposition of the homogeneous ZnO compact layer.

### 2.3 Preparation of paste

1 g ZnO nanopowders were dispersed in 15 mL ethanol under sonication for 1 hr. Ethyl cellulose was added as a pore-filling agent and a few mL of terpinol was added in the above suspension. After that, half mL of acetylacetone was added in it. The paste was collected in a bottle and placed in an incubator air to remove excess ethanol until the slurry paste was obtained. Following the same steps, In<sub>2</sub>O<sub>3</sub> paste was prepared.

### 2.4 Preparation of photoanodes and device fabrication

Initially, a layer of compact ZnO on FTO was prepared by the SILAR method. A ZnO layer was deposited by the doctor blade technique, followed by an indium oxide layer. Thus, a bilayer film (ZnO compact/ZnO/In<sub>2</sub>O<sub>3</sub>) was fabricated. The prepared films were dried at 60 °C in an incubator for about 25-30 min. The prepared film was placed in a glass petri dish. The temperature of the furnace was set at 450 °C. The films were annealed at 450 °C in the furnace for about 1 h. 25 mL, 1 mM solution of MC photosensitizers were prepared in ethanol separately. The ZnO/In<sub>2</sub>O<sub>3</sub> photoanode was immersed in these photosensitizers solutions for 36 hrs for the sensitization of photosensitizers. Then sensitized photoanodes were clean with ethanol and taken for further characterization. The DSSCs devices were fabricated using MC photosensitizers sensitized ZnO/In<sub>2</sub>O<sub>3</sub> photoanode, poly-iodide as the electrolyte, and platinumized FTO coated substrate as the counter electrode.

### 3. Characterization and measurements

The optical, morphological, and structural properties of prepared ZnO, In<sub>2</sub>O<sub>3</sub>, and ZnO/In<sub>2</sub>O<sub>3</sub> electrodes were characterized by different techniques such as UV-Visible spectroscopy, scanning electron microscopy (SEM) and X-ray diffraction technique (XRD), etc. Optical properties of prepared ZnO, In<sub>2</sub>O<sub>3</sub>, and ZnO/In<sub>2</sub>O<sub>3</sub> electrodes were investigated by JASCO V-670 UV-Vis spectrophotometer. The surface morphology of deposited ZnO/In<sub>2</sub>O<sub>3</sub> bilayer was characterized by using JSM-7600F. The structural parameters like crystal structure, crystallite size and crystal orientation were investigated using an X-ray diffractometer model Bruker D8 with Cu K<sub>α</sub> radiation of wavelength 1.54 Å. The photovoltaic performances of ZnO/ In<sub>2</sub>O<sub>3</sub> bilayer were studied by using a Keithley 2400 source meter and solar simulator (ENLITECH Model SS-F5-3A) under one sun condition.

## 4. Results and discussion

### 4.1 Structural properties

The structural properties of the material were studied with the help of X-ray diffraction. The system recorded the intensity as a function of Bragg's angle. Crystal structures of

films were analyzed by using an X-ray diffractometer with Cu K<sub>α</sub> target, with a radiation wavelength ( $\lambda=1.5406 \text{ \AA}$ ) and scanning angle ( $2\theta=20^\circ-80^\circ$ ). Fig. 3 shows the XRD patterns of ZnO, In<sub>2</sub>O<sub>3</sub>, and ZnO/In<sub>2</sub>O<sub>3</sub> bilayer. According to JCPDS card no: 36-1451,<sup>[34]</sup> the peak obtained at  $2\theta=31.82^\circ$  with (100) confirms the hexagonal wurtzite crystal structure of ZnO.<sup>[35]</sup> The peak obtained at  $2\theta=30.62^\circ$  with (222) confirms the cubic crystal structure of In<sub>2</sub>O<sub>3</sub>,<sup>[36]</sup> with JCPDS card no: 06-046.<sup>[37]</sup> From the JCPDS data, we confirm that ZnO shows hexagonal wurtzite crystal structure, with a crystallite size 34.85 nm and the lattice parameter corresponds to  $a=3.24 \text{ \AA}$ ,  $b=5.20 \text{ \AA}$ ,  $c=1.60 \text{ \AA}$  and that of In<sub>2</sub>O<sub>3</sub> shows cubic crystal structure, with a crystallite size of 40.17 nm and the lattice parameter are  $a=b=c=10.11 \text{ \AA}$ , respectively. The sharp intensity peaks indicate the high crystallinity of the bilayer than individual ZnO and In<sub>2</sub>O<sub>3</sub>.

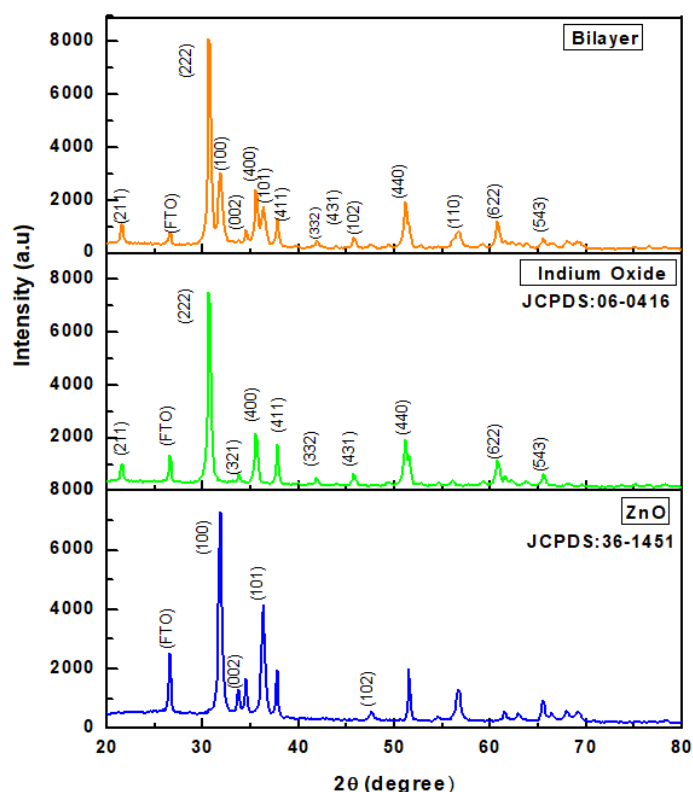


Fig. 3 XRD pattern of ZnO, In<sub>2</sub>O<sub>3</sub>, and ZnO/In<sub>2</sub>O<sub>3</sub> bilayer respectively.

### 4.2 Optical properties

UV-Visible spectroscopy was used to study the optical properties of zinc oxide, indium oxide and ZnO/In<sub>2</sub>O<sub>3</sub> bilayer. The absorption spectrum of ZnO, In<sub>2</sub>O<sub>3</sub> and bilayer is recorded in the range of 300-800 nm wavelength. Fig. 4 shows the absorption spectra and Fig. 5 shows the tauc plot of ZnO, In<sub>2</sub>O<sub>3</sub>, and ZnO/ In<sub>2</sub>O<sub>3</sub> bilayer. The absorption spectra clearly show that an optical band situated at 300-390 nm for ZnO, 300-400 nm for In<sub>2</sub>O<sub>3</sub> and 300-500 nm for bilayer. UV-visible spectra show that the ZnO/ In<sub>2</sub>O<sub>3</sub> bilayer film absorbs a larger region of UV and visible radiation as compared to individual ZnO and In<sub>2</sub>O<sub>3</sub> film. The bandgap of

ZnO, In<sub>2</sub>O<sub>3</sub> and bilayer were found to be 3.2, 2.87 and 2.95 eV, respectively.<sup>[28,38]</sup>

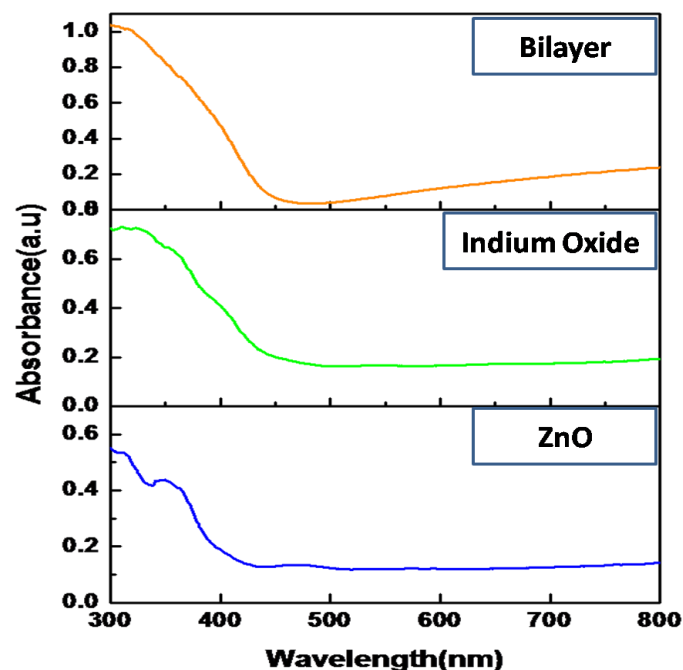


Fig. 4 UV-Visible absorption spectra of ZnO, In<sub>2</sub>O<sub>3</sub> and ZnO/In<sub>2</sub>O<sub>3</sub> photoanode.

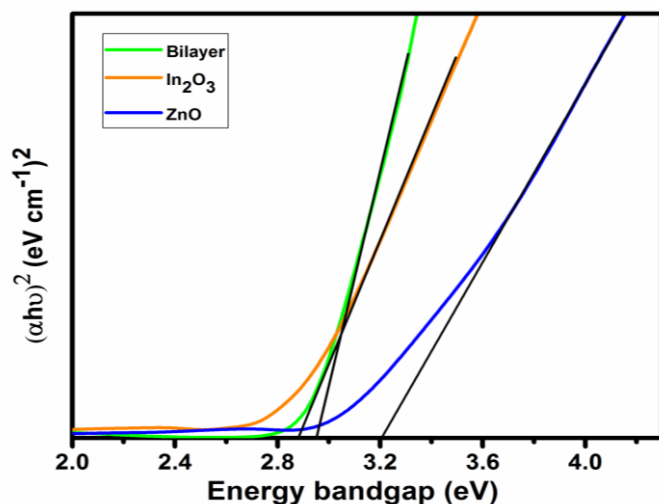


Fig. 5 Tauc plot of ZnO, In<sub>2</sub>O<sub>3</sub>, and ZnO/In<sub>2</sub>O<sub>3</sub> bilayer photoanodes.

### 4.3 Morphological properties

Fig. 6 shows surface morphology of compact ZnO/ZnO/In<sub>2</sub>O<sub>3</sub> bilayer film. It shows the porous nature of bilayer. If we can fabricate a porous film, a good amount of dye will get loaded into it. So it is very essential to get a porous nature of the film.<sup>[39]</sup> The high porosity of bilayer film is responsible for the absorption of more dye molecules as compared to individual ZnO and In<sub>2</sub>O<sub>3</sub> layer. Hence photoconversion efficiency of the device is enhanced. The thickness of the bilayer was calculated by SEM cross-section with the help of Image J software. Fig. 7 shows the SEM cross-section of bilayer film. The thickness of compact ZnO was found to be

1.6 μm and that of ZnO and In<sub>2</sub>O<sub>3</sub> was found to be 3.51, and 4.17 μm respectively. The total film thickness was found to be 9.28 μm.

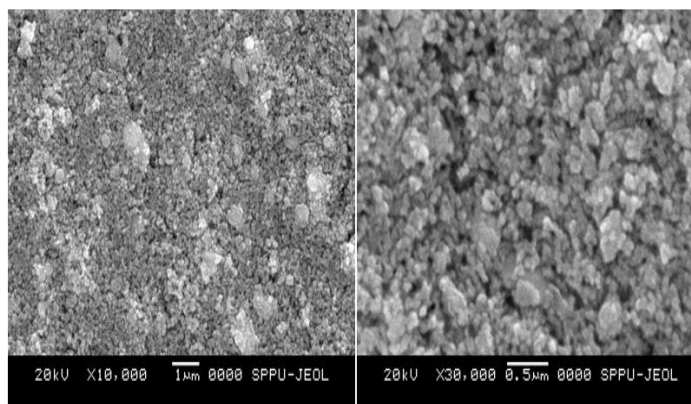


Fig. 6 SEM images of synthesized compact ZnO/ZnO/In<sub>2</sub>O<sub>3</sub> bilayer at various magnifications.

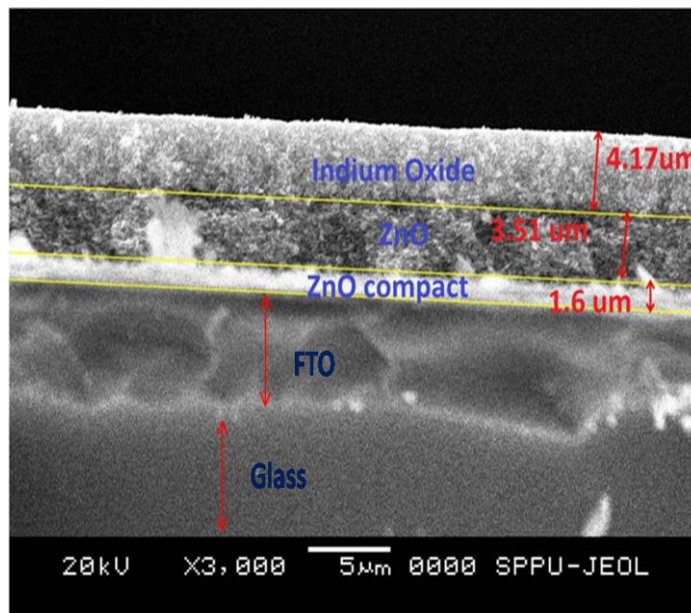


Fig. 7 SEM cross-section image of compact ZnO/ZnO/In<sub>2</sub>O<sub>3</sub> bilayer film.

### 4.4 Photovoltaic properties

Fig. 8 shows the photovoltaic curve of the MC sensitized ZnO, In<sub>2</sub>O<sub>3</sub>, and ZnO/ In<sub>2</sub>O<sub>3</sub> bilayer based DSSC. All the photoanodes were sensitized with MC sensitizer at the same dye loading time. *J-V* characteristics of the device were tested under one sun condition (100 mW/cm<sup>2</sup>). The values of fill factor (*FF*) were calculated using Equation (1).<sup>[40]</sup>

$$FF = P_{max}/(I_{sc} \times V_{oc}) \quad (1)$$

where *V<sub>oc</sub>* and *I<sub>sc</sub>* are open circuit voltage and short circuit current. *P<sub>max</sub>* is the maximum power delivery point. The photoelectric conversion efficiency (*η*) of DSSC is calculated using Equation (2):<sup>[40]</sup>

$$\eta = (I_{sc} \times V_{oc})/P_{in} \times FF \quad (2)$$

where *P<sub>in</sub>* is the incident light power.

**Table 1.** Photovoltaic parameters of MC sensitized ZnO, In<sub>2</sub>O<sub>3</sub>, and ZnO/In<sub>2</sub>O<sub>3</sub> bilayer photoanode based DSSCs.

Photoanode	dye	$V_{oc}$ (mV)	$J_{sc}$ (mA cm <sup>-2</sup> )	$FF$	Efficiency (%)
ZnO	MC	0.56	2.57	25.25	0.36
In <sub>2</sub> O <sub>3</sub>		0.37	1.23	20.52	0.09
ZnO/In <sub>2</sub> O <sub>3</sub> Bilayer		0.43	3.44	34.7	0.51

Photovoltaic parameters like open-circuit voltage ( $V_{oc}$ ), short-circuit photocurrent density ( $J_{sc}$ ), fill factor ( $FF$ ) and photovoltaic efficiency ( $\eta$ ) are summarized in Table 1.

From the  $J$ - $V$  characteristics, the photoconversion efficiency of MC sensitized ZnO, In<sub>2</sub>O<sub>3</sub> and ZnO/ In<sub>2</sub>O<sub>3</sub> bilayer photoanode based DSSCs were found to be 0.36, 0.09, and 0.51, respectively. Zhang *et al.* achieved  $V_{oc}$  of 0.34 V for In<sub>2</sub>O<sub>3</sub> based DSSC, which was exactly similar to our result. Since it adsorbs the reactant molecules with low amount energies and it also limits the active sites of the adsorbing reactants.<sup>[29]</sup> Eguchi *et al.* fabricated N3 sensitized In<sub>2</sub>O<sub>3</sub> based DSSC by the doctor blade method; and achieved 0.029 % efficiency, which was smaller than the photoconversion efficiency of our In<sub>2</sub>O<sub>3</sub> based DSSC.<sup>[30]</sup> An additional layer of In<sub>2</sub>O<sub>3</sub> on the ZnO layer is attributed to enhance dye absorption rate and reduce the electron recombination rate. This is responsible for the improvement in the photoconversion efficiency of the device.<sup>[32]</sup> A similar study carried out by Beedri *et al.*<sup>[33]</sup> reporting that an additional layer of Nb<sub>2</sub>O<sub>5</sub> enhances the performance of ZnO based DSSCs.

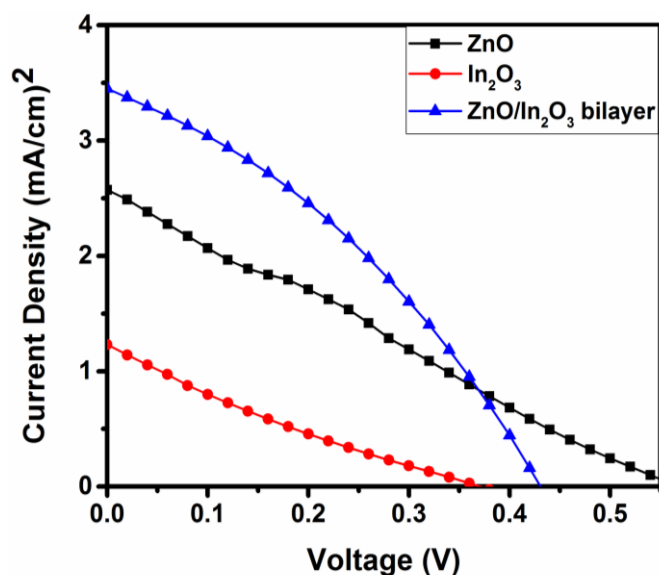


**Fig. 8**  $J$ - $V$  characteristics of MC sensitized ZnO, In<sub>2</sub>O<sub>3</sub>, and ZnO/In<sub>2</sub>O<sub>3</sub> bilayer photoanode based DSSCs.

## 5. Conclusion

In the present study, we have successfully fabricated a novel MC sensitized ZnO/ In<sub>2</sub>O<sub>3</sub> photoanode based Dye-Sensitized Solar cell. XRD pattern confirmed the hexagonal wurtzite crystal structure of ZnO and a cubic crystal structure of In<sub>2</sub>O<sub>3</sub>. The average crystallite size of the bilayer was found to be 31.80 nm. The crystallinity of the bilayer film is better than that of individual ZnO and In<sub>2</sub>O<sub>3</sub> layers. SEM image confirmed the porous nature of the film, which indicates that the loading of dye will be greater in bilayer as compare to that of individual ZnO and In<sub>2</sub>O<sub>3</sub>. Optical spectra confirmed that visible light absorption of the ZnO/In<sub>2</sub>O<sub>3</sub> bilayer photoanode is more effective than bare ZnO and In<sub>2</sub>O<sub>3</sub> photoanodes. A 0.51 % photoconversion efficiency has been achieved for MC sensitized ZnO/ In<sub>2</sub>O<sub>3</sub> bilayered photoanode based DSSC. An additional layer of In<sub>2</sub>O<sub>3</sub> on the ZnO layer is responsible for the improvement in the photoconversion efficiency of the device. Hence we confirmed that ZnO/In<sub>2</sub>O<sub>3</sub> bilayer photoanode based DSSCs shows better performance than single-layered ZnO and single-layered In<sub>2</sub>O<sub>3</sub> based DSSCs. Finally, we conclude that ZnO/In<sub>2</sub>O<sub>3</sub> bilayer photoanode is a potential and cost-effective alternative to the ZnO based DSSCs.

## Acknowledgment

HMP acknowledge the Department of Science and Technology, Government of India for financial support vide Sanction order DST/TMD/SERI/S173 (G).

## Supporting information

Not applicable

## Conflict of interest

There are no conflicts to declare.

## References

- [1] E. Stathatos, *Solar cells-dye-sensitized devices*, 2011, 471-492, doi: 10.5772/23650
- [2] C. P. Lee, C. T. Li and K. C. Ho, *Mater. Today*, 2017, **20**, 267-283, doi:10.1016/j.mattod.2017.01.012.
- [3] A. F. Husain, W. W. Hasan, S. Shafie, M. Hamidon and S. Pandey, *Renew. Sust. Energ. Rev.*, 2018, **94**, 779-791, doi: 10.1016/j.rser.2018.06.031.
- [4] M. Freitag, J. Teuscher, Y. Saygili, X. Zhang, F. Giordano, P. Liska, J. Hua, S. Zakeeruddin, J. Moser, M. Grätzel and A. Hagfeldt, *Nat. Photonics*, 2017, **11**, 372-378, doi: 10.1038/nphoton.2017.60.
- [5] M. Grätzel, *J. Photoch. Photobio. C*, 2003, **4**, 145-153, doi: 10.1016/S1389-5567(03)00026-1.
- [6] N. Kamarulzaman, M. Kasim and R. Rusdi, *Nanoscale Res. Lett.*, 2015, **10**, 346, doi: 10.1186/s11671-015-1034-9.
- [7] E. Monroy, F. Omnès and F. Calle, *Semicond. Sci. Tech.*, 2003, **18**, R33-R51, doi: 10.1088/0268-1242/18/4/201.
- [8] D. Zhao, T. Peng, L. Lu, P. Cai, P. Jiang and Z. Bian, *J. Phys. Chem. C*, 2008, **112**, 8486-8494, doi: 10.1021/jp800127x.

- [9] Z. S. Wang, H. Kawauchi, T. Kashima and H. Arakawa, *Coord. Chem. Rev.*, 2004, **248**, 1381-1389, doi: 10.1016/j.ccr.2004.03.006.
- [10] Y. Alivov and Z. Y. Fan, *J. Mater. Sci.*, 2010, **45**, 2902-2906, doi: 10.1007/s10853-010-4281-2.
- [11] U. Bach, D. Lupo, P. Comte, J. E. Moser, F. Weissörtel, J. Salbeck, H. Spreitzer and M. Grätzel, *Nature*, 1998, **395**, 583-585, doi: 10.1038/26936.
- [12] D. Lee, S. Jang, R. Vittal, J. Lee and K. Kim, *Sol. Energy*, 2008, **82**, 1042-1048, doi: 10.1016/j.solener.2008.04.006.
- [13] R. Kumar, A. Umar, G. Kumar, H. Nalwa, A. Kumar and M. Akhtar, *J. Mater. Sci.*, 2017, **52**, 4743-4795, doi: 10.1007/s10853-016-0668-z.
- [14] A. Le Viet, R. Jose, M. Reddy, B. Chowdari and S. Ramakrishna, *J. Phys. Chem. C*, 2010, **114**, 21795-21800, doi: 10.1021/jp106515k.
- [15] H. Elbohy, K. M. Reza, S. Abdulkarim and Q. Qiao, *Sustainable Energy Fuels*, 2018, **2**, 403-412, doi: 10.1039/c7se00483d.
- [16] S. Chappel and A. Zaban, *Sol. Energy Mater. Sol. Cells*, 2002, **71**, 141-152, doi: 10.1016/S0927-0248(01)00050-2.
- [17] Y. Fukai, Y. Kondo, S. Mori and E. Suzuki, *Electrochem. Commun.*, 2007, **9**, 1439-1443, doi: 10.1016/j.elecom.2007.01.054.
- [18] M. Quintana, T. Marinado, K. Nonomura, G. Boschloo and A. Hagfeldt, *J. Photochem. Photobiol. A Chem.*, 2009, **202**, 159-163, doi: 10.1016/j.jphotochem.2008.11.024.
- [19] I. Concina and A. Vomiero, *Small*, 2015, **11**, 1744-1774, doi: 10.1002/sml.201402334.
- [20] R. Mane, W. J. Lee, H. M. Pathan and S. H. Han, *J. Phys. Chem. B*, 2005, **109**, 24254-24259, doi: 10.1021/jp0531560.
- [21] O. Ola and M. Maroto-Valer, *J. Photochem. Photobiol. C*, 2015, **24**, 16-42, doi: 10.1016/j.jphotochemrev.2015.06.001.
- [22] K. Qi, B. Cheng, J. Yu and W. Ho, *J. Alloy. Compd.*, 2017, **727**, 792-820, doi: 10.1016/j.jallcom.2017.08.142.
- [23] Pankaj K. Bhujbal, Habib M. Pathan and Nandu B. Chaure, *ES Energy Environ.*, 2019, **4**, 15-18, doi: 10.30919/ese8c188.
- [24] Pankaj K. Bhujbal, Habib M. Pathan and Nandu B. Chaure, *Eng. Sci.*, 2020, **10**, 58-67, doi: 10.30919/es8d1003.
- [25] Y. Dou, F. Wu, C. Mao, L. Fang, S. Guo and M. Zhou, *J. Alloy. Compd.*, 2015, **633**, 408-414, doi: 10.1016/j.jallcom.2015.02.039.
- [26] R. Kumar, A. Umar, G. Kumar, H. S. Nalwa, A. Kumar and M. S. Akhtar, *J. Mater. Sci.*, 2017, **52**, 4743-4795, doi: 10.1007/s10853-016-0668-z.
- [27] A. Aprilia, L. Safriani, W. Arsyad, N. Syakir, T. Susilawati, C. Mulyana and R. Fitrilawati, *IOP Conf. Series, Mater. Sci. Eng.*, 2017, **214**, 012033, doi: 10.1088/1757-899X/214/1/012033.
- [28] S. Sanctis, J. Krausmann, C. Guhlb and J. Schneider, *J. Mater. Chem. C*, 2018, **6**, 464-472, doi: 10.1039/c7tc03724d.
- [29] B. Zhang, N. N. Zhang, J. Chen, Y. Hou, S. Yang, J. Guo, X. Yang, J. Zhong, H. Wang, P. Hu, H. Zhao and H. Yang, *Sci. Rep.*, 2013, **3**, 3109, doi: 10.1038/srep03109.
- [30] K. Eguchi, H. Koga, K. Sekizawa and K. Sasaki, *J. Ceram. Soc. Jpn.*, 2000, **108**, 1067-1071, doi: 10.2109/jcersj.108.1264\_1067.
- [31] S. Mahalingam and H. Abdullah, *Renew. Sust. Energ. Rev.*, 2016, **63**, 245-255, doi: 10.1016/j.rser.2016.05.067.
- [32] N. Huu, D. Son, I. H. Jang, C. Lee and N. Park, *ACS Appl. Mater. Inter.*, 2013, **5**, 1038-1043, doi: 10.1021/am302729v.
- [33] N. I. Beedri, P. K. Baviskar, A. T. Supekar, Inamuddin, S. R. Jadkar and H. M. Pathan, *Int. J. Mod. Phys. B*, 2018, **32**, 1840046, doi: 10.1142/S0217979218400465.
- [34] H. Mokhtar, Lassaad El Mir, Salvatore Gianluca Leonardi, Nicola Donato and Giovanni Neri, *Nanomaterials*, 2013, **3**, 357-369, doi: 10.3390/nano3030357.
- [35] N. F. Hamedani and F. Farzaneh, *J. Sciences, Islamic Republic of Iran*, 2006, **17**, 231-234.
- [36] M. Thirumoorthi and J. Thomas Joseph Prakash, *J. Asian Ceram. Soc.*, 2016, **4**, 124-132, doi: 10.1016/j.jascer.2016.01.001.
- [37] J. Xu, X. Wang, G. Wang, J. Han and Y. Sun, *Electrochem. Solid State*, 2006, **9**, H103-H107, doi: 10.1149/1.2335943.
- [38] S. Trevizo, P. Madrid, P. Ruiz, W. Flores and M. Yoshida, *Mater. Res.*, 2016, **19**, 33-38, doi: 10.1590/1980-5373-MR-2015-0612.
- [39] M. Giannouli and F. Spiliopoulou, *Renew. Energ.*, 2012, **41**, 115-122, doi: 10.1016/j.renene.2011.10.010.
- [40] M. Giannouli, K. Govatsi, G. Syrokostas, S. N. Yannopoulos and G. Leftheriotis, *Materials*, 2018, **11**, 411, doi: 10.3390/ma11030411.

**Publisher's Note:** Engineered Science Publisher remains neutral with regard to jurisdictional claims in published maps and institutional affiliations.